Physica E 42 (2010) 1216–1219

Contents lists available at ScienceDirect

Physica E

journal homepage: www.elsevier.com/locate/physe

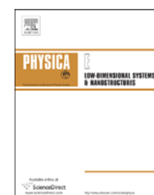

A voltage-tunable in-plane diode in a two-dimensional-electron system

A. Ganczarczyk [a,*], S. Voßen [a], M. Geller [a], A. Lorke [a], D. Reuter [b], A.D. Wieck [b]

[a] Experimental Physics and CeNIDE, Universität Duisburg-Essen, Lotharstraße 1, 47048 Duisburg, Germany
[b] Chair of Applied Solid State Physics, Ruhr-Universität Bochum, Universitätsstraße 150, 44780 Bochum, Germany

ARTICLE INFO

Available online 22 October 2009

Keywords:
Electron gases
Rectification
In-plane diode
Self-switching effect

ABSTRACT

We present a voltage-tunable in-plane diode in a nanoscale, two-dimensional electron system, whose functionality is mainly determined by the sample geometry. The diode consists of a narrow semiconductor channel, confined by etched insulating trenches. An applied voltage along the channel modulates the effective width of the conducting channel, depending on the sign of the applied voltage. This behavior results in a diode-like $IV-$characteristic. The tunability of the device is achieved by two in-plane side gates, which are able to widely tune the $I(V)-$characteristic of this rectifier. In the normally-off regime, this tunable in-plane diode works as a half-wave rectifier with sharply defined turn-on voltage. The value of the turn-on voltage depends on the side-gate voltage.
© 2009 Elsevier B.V. All rights reserved.

1. Introduction

Advances in lithography have made it possible to reduce the dimensions of semiconductor devices to the nanometer scale. These advances were the basis for the considerable growth of the semiconductor industry in the past decades. Furthermore, the improvements in both materials and nanofabrication have led to the development of radically new device concepts. Examples are ballistic rectifiers [1–5] and $y-$branches [6–11], whose transport properties are mainly determined by the sample geometry rather than material composition. These devices make use of effects, such as ballistic transport or quantized conductance, which become dominant at the nanometer scale. They often have the advantage of simple device fabrication and working principles. Another way to make use of a nanoscale patterning is to choose a device geometry, where the applied voltage, which drives the current in the device, influences itself. These devices are called self-gating or self-switching devices [7,10,12–14].

Recently, Song et al. presented a self-switching in-plane diode [15], capable of rectification at room temperature [16] or up to the THz regime [17,18]. This device uses an electron channel defined by two L-shaped trenches. This geometry translates the bias along the channel into a lateral side gate voltage (similar to the in-plane-gate devices, introduced by Wieck et al. [19,20]). Depending on the polarity of the bias, the channel will open or close, leading to a self-switching, diode-like behavior.

Here, we further develop the concept of the in-plane diode by extending the etched trenches and thus completely separating the side-gates from the electron channel. This results in additional electrical tunability of the channel width and makes it possible to widely adjust the device characteristics. $I(V)-$traces similar to those observed by Song et al. can be realized as well as rectification characteristics similar to those of a conventional p–n-diode. Furthermore, the sharply defined turn-on voltage can be tuned, resulting in a small signal voltage discriminator with an adjustable threshold.

2. Material and methods

The investigated samples are fabricated from a modulation-doped $GaAs/Al_{0.34}Ga_{0.66}As$ heterostructure, grown by molecular beam epitaxy. The heterostructure contains a two-dimensional electron gas (2DEG), situated 80 nm below the surface. The sheet charge carrier density and mobility at a temperature of $T = 4.2$ K are $3 \times 10^{15}\,m^{-2}$ and $100\,m^2/V\,s$, respectively. Optical lithography and successive wet chemical etching is used to define the macroscopic, cross shaped mesa structure (see Fig. 1). Ohmic contacts are made of Ni/AuGe/Au layers formed by high-vacuum deposition and successive thermal annealing.

The 300 nm wide insulating trenches are defined by electron beam lithography and reactive plasma etching. The resulting electron channel has a length of 5 μm and a geometrical width of 430 nm. A scanning electron microscope (SEM) image of the in-plane diode is shown in Fig. 1. The channel voltage V_{AB} is applied at terminal A, with respect to the grounded terminal B and the channel current I_{AB} between these terminals is measured. The gate voltage V_G is applied to the two side-gates with respect to the potential at the $A-$terminal. The whole mesa-structure has a length of 750 μm and a width of 60 μm. All measurements are performed at 4.2 K.

* Corresponding author. Tel.: +492033792867; fax: +492033792709.
E-mail address: arkadius.ganczarczyk@uni-due.de (A. Ganczarczyk).

1386-9477/$ - see front matter © 2009 Elsevier B.V. All rights reserved.
doi:10.1016/j.physe.2009.10.018

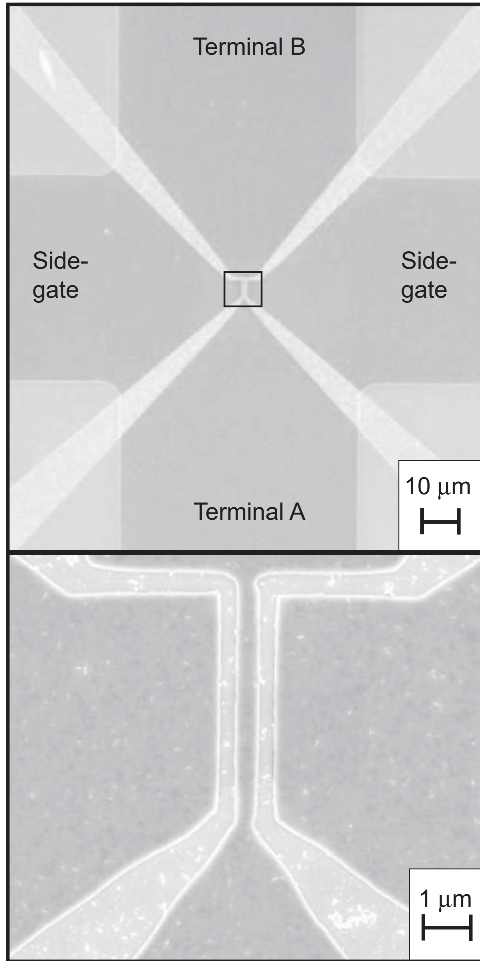

Fig. 1. SEM images of the in-plane diode: top: the dark-gray colored area represents the 2DEG and the etched insulating trenches are light-gray colored and bottom: magnified view of the area indicated by the rectangle in the top image.

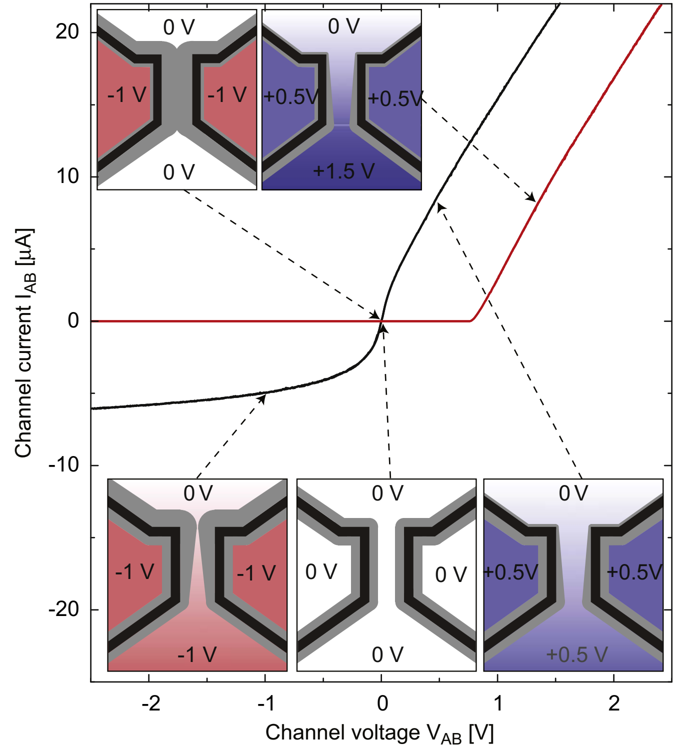

Fig. 2. Channel current I_{AB} as function of the applied channel voltage V_{AB} for a gate-voltage of $V_G = 0\,V$ (black trace) and $V_G = -1\,V$ (red trace). The insets show the potential gradient in the channel and the extension of the depletion zones for different channel and gate voltages. The insets for unbiased gates are shown in the bottom of the figure, while the insets for the biased gates are shown in the top. The etched trenches are illustrated in black color and the depletions zones are indicated in gray. Red and blue color correspond to a negative and positive potential, respectively, while white represents the unbiased state. (For interpretation of the references to the color in this figure legend, the reader is referred to the web version of this article.)

3. Results and discussion

Fig. 2 shows the channel current I_{AB} as a function of the applied channel voltage V_{AB} for two different gate-voltages. For a gate-voltage of $V_G = 0\,V$ (black trace), the conductive channel of the device is open for $V_{AB} = 0\,V$: the tunable diode is in the normally on state with a comparably low resistance. With decreasing channel voltage V_{AB}, the differential resistance increases and the channel current shows a saturation behavior at about $I_{AB} = -6\,\mu A$. Thus, the channel of the device closes for negative channel voltages (reverse direction). For positive channel voltages the channel opens (conducting direction) and the current increases approximately linearly with the applied channel voltage. For a gate voltage of $V_G = -1\,V$ (red trace), the channel is completely closed at a channel voltage of $V_{AB} = 0\,V$: the device has switched into the normally off state. No current flow is visible up to a turn-on voltage of $V_T \approx 0.7\,V$. Above the turn-on voltage V_T, the current increases linearly. The $I(V)$–characteristic with biased side-gates shows an almost perfect half-wave rectification behavior with a sharply defined turn-on voltage.

These $I(V)$–characteristic can be explained with the help of the insets of Fig. 2. We assume in the following a linear gradient of the potential inside the conducting channel between terminal A and B. Sophisticated Monte-Carlo simulations predict a non-linear potential landscape inside the channel [21], however, a linear approximation is sufficient for the understanding of the device operation. The situation for the unbiased state ($V_{AB} = 0\,V$ and $V_G = 0\,V$) is shown in the inset (d). The channel is open, because the total width of the depletion zones is smaller than the channel width at any point along the channel. The situation for a negative channel voltage V_{AB} can be seen in the inset (c) of Fig. 2. Note that, as the gate-voltage $V_G = 0\,V$ is applied with respect to the potential at the terminal A, the potential at the side-gates matches the potential at the A–terminal. However, close to the B–terminal, the local potential difference V_{diff} between the side-gates and the channel is negative, resulting in an increased width of the depletion zones and consequently an increased resistance of the channel. This leads to the observed saturation behavior in the $I(V)$–characteristic in the reverse direction. The situation changes when a positive channel voltage V_{AB} is applied (see in inset (e) of Fig. 2). The potential difference V_{diff} is now positive close to terminal B, which causes a decreasing width of the depletion zones. The resistance in the upper half of the channel decreases, while the resistance remains constant in the lower half of the channel. The resistance in the lower half of the channel dominates the resistance of the entire channel and a roughly linear increase of the channel current I_{AB} with the applied channel voltage V_{AB} is observed.

The tunable diode can be set into a normally off state—similar to the situation studied by Song et al.—by applying a side-gate voltage $V_G = -1\,V$. The negative side-gate voltage leads to an increase of the depletion zones in the channel and the electron channel becomes completely depleted for $V_{AB} = 0\,V$ (see inset (a)

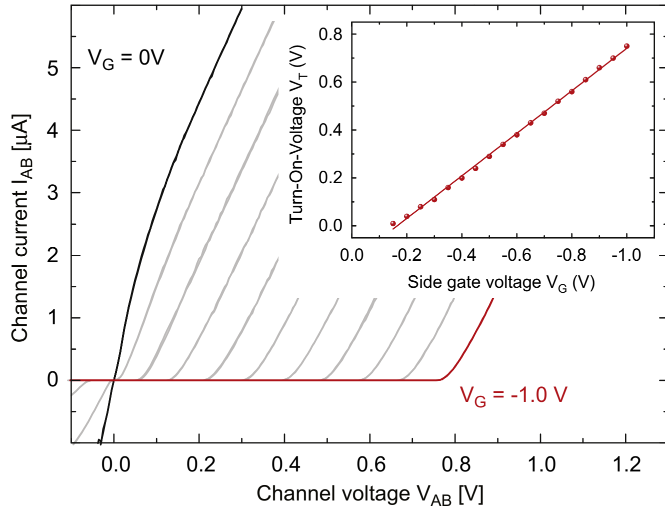

Fig. 3. The turn-on voltage V_T of the $I(V)$–traces for side-gate voltages from $V_G = 0$ V (black trace) to $V_G = -1$ V (red trace) in steps of 0.1 V. The inset shows the turn-on-voltage V_T in dependence on the side-gate voltage V_G. (For interpretation of the references to the color in this figure legend, the reader is referred to the web version of this article.)

in Fig. 2). An applied negative channel voltage increases the depletion zones even further, so that the channel of the diode remains closed. Positive voltages V_{AB} decrease the width of the depletion zones and above a certain turn-on voltage V_T the channel of the tunable diode opens, as schematically depicted in the inset (b) of Fig. 2.

Fig. 3 further demonstrates the voltage tunability of the device. The $I(V)$–characteristic of the diode is shown for positive channel voltages and for gates voltages ranging from $V_G = 0$ V (black trace) to $V_G = -1$ V (red trace) in steps of 0.1 V. For a gate-voltage V_G between ≈ -0.15 and -1 V the tunable diode operates in the normally-off state with sharply defined turn-on voltages V_T ranging from 0 V up to ≈ 0.75 V. At the turn-on voltage, the channel opens and the current increases linearly with the applied channel voltage. The inset of Fig. 3 shows the turn-on voltage V_T as a function of the side-gate voltage V_G. We find that the turn-on voltage of the diode depends linearly on the side-gate voltage V_G with a slope of ≈ 0.9. The observation, that the turn-on voltage depends linearly on the side-gate voltage, is in good agreement with previous experiments, e.g. of Reuter et al. [22]. They investigated the depletion characteristics of two-dimensional lateral p–n-junctions and found the following dependence between the depletion width L_{depl} and the reverse bias V:

$$L_{depl} = \frac{\varepsilon_0 \varepsilon_r}{e n_s}(V_{bi} - V).$$

Here, V_{bi} is the built-in potential of the p–n-junction and ε_r the effective dielectric constant. These results are supported by the theoretical considerations of Achoyan et al. [23]. They show, that the Schottky approximation can be used for a description of the properties of such p–n-junctions and use it to derive the above equation.

The inset of Fig. 3 shows that the side-gate voltage $V_{G0} \approx -0.15$ V can be used to set the tunable diode from the normally on state in the normally off state. At this point, the turn-on voltage is $V_T = 0$ V and the diode is able to rectify even very small signals, a situation, which is impossible for conventional diodes, where the curvature at low bias is given by the Schottky equation. Generally, the side-gate voltage V_{G0}, needed to close the channel, can easily be adjusted by an appropriate choice of the etched channel width and the material properties of the device, which determine the width of the depletion zones [24].

The well defined and widely tunable turn-on voltage and the ideal half-wave rectification behavior of the device for negative side-gate voltages allows many interesting applications. We demonstrate here the use of the diode as a voltage discriminator. Signals below a certain threshold voltage (i.e. the turn-on voltage) are ignored, while input voltages above this threshold are registered. This behavior is shown in Fig. 4, where the channel current I_{AB} (red trace) is plotted for a sinusoidal channel voltage V_{AB} (black trace) with frequency and amplitude of 1 kHz and 1.5 V, respectively. The green dotted line marks the turn-on voltage V_T as determined from Fig. 3.

Fig. 4 shows a full period (1 ms) of the input and output signals for side-gate voltages $V_G = 0$, -0.5 and -0.9 V. At a side-gate voltage of $V_G = 0$ V, the channel current I_{AB} is proportional to the channel voltage V_{AB} for the positive half-wave (conducting direction) and almost completely vanishes for the negative half-wave, as expected from the IV–characteristics in Fig. 2. This behavior is even more pronounced for a side-gate voltage of $V_G = -0.5$ V, where the channel current is now zero for the negative half-wave. For the positive half-wave the channel remains closed up to the turn-on voltage V_T. Only the input voltages above the turn-on voltage are registered and the device now functions as a voltage discriminator. A side-gate voltage $V_G = -0.9$ V yields a similar behavior of the in-plane diode, only

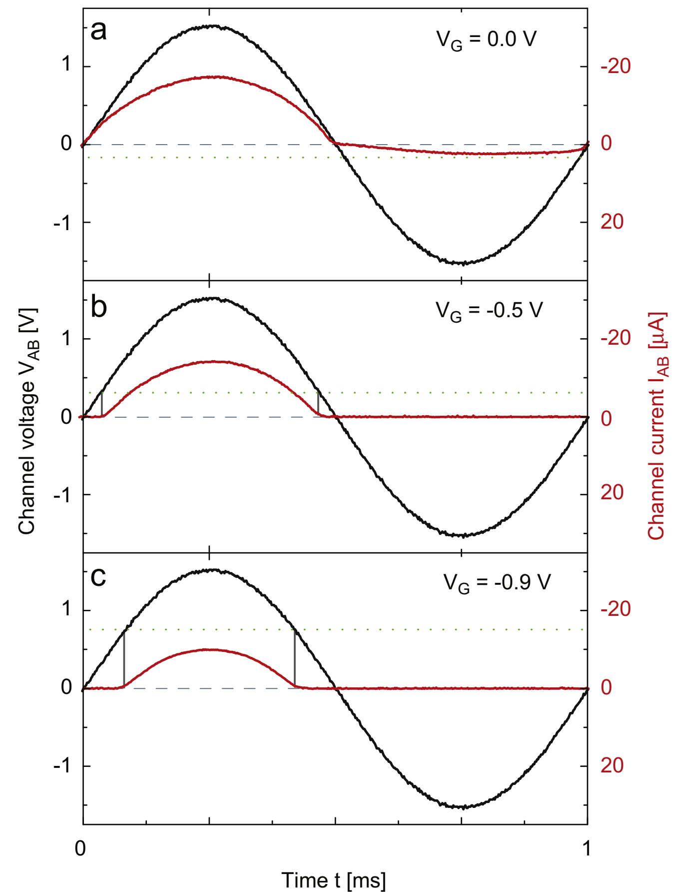

Fig. 4. Channel current I_{AB} as a function of the channel voltage V_{AB}. A sinusoidal input signal with a frequency of 1 kHz was applied for side-gate voltages of (a) $V_G = 0$ V, (b) $V_G = -0.5$ V and (c) $V_G = -0.9$ V. The black traces show the sine-wave input signal, while the channel current is represented by the red traces. The dotted green line marks the turn-on voltage V_T for a given side-gate voltage V_G. (For interpretation of the references to the color in this figure legend, the reader is referred to the web version of this article.)

with a turn-on voltage of $V_T = 0.75\,\mathrm{V}$. The voltage discrimination works up to a cutoff frequency of $\approx 30\,\mathrm{kHz}$, presently limited by the parasitic RC element.

4. Conclusions

In conclusion, we demonstrate a voltage-tunable in-plane diode in a two-dimensional-electron-system. For unbiased gates, the tunable diode operates in the normally on state and shows $I(V)-$characteristic similar to a conventional p–n-diode. For negative gate voltages below a gate voltage V_{G0} the device operates in the normally off state, with sharply defined turn-on voltage. In this regime the device functions as a perfect half-wave rectifier or voltage discriminator, which is also suitable for small signals.

Acknowledgment

We acknowledge financial support by the BMBF via the nanoQUIT program.

References

[1] A.M. Song, A. Lorke, A. Kriele, J.P. Kotthaus, W. Wegscheider, M. Bichler, Phys. Rev. Lett. 80 (1998) 3831.
[2] A. Lofgren, I. Shorubalko, P. Omling, A.M. Song, Phys. Rev. B 67 (2003) 195309.
[3] S. de Haan, A. Lorke, J.P. Kotthaus, W. Wegscheider, M. Bichler, Phys. Rev. Lett. 92 (2004) 56806.
[4] B. Hackens, L. Gence, C. Gustin, X. Wallart, S. Bollaert, A. Cappy, V. Bayot, Appl. Phys. Lett. 85 (2004) 4508.
[5] M. Knop, U. Wieser, U. Kunze, D. Reuter, A.D. Wieck, Appl. Phys. Lett. 88 (2006) 082110.
[6] T. Palm, L. Thylen, Appl. Phys. Lett. 60 (1992) 237.
[7] K. Hieke, M. Ulfward, Phys. Rev. B 62 (2000) 16727.
[8] C. Papadopoulos, A. Rakitin, J. Li, A. Vedeneev, J. Xu, Phys. Rev. Lett. 85 (2000) 3476.
[9] L. Worschech, H. Xu, A. Forchel, L. Samuelson, Appl. Phys. Lett. 79 (2001) 3287.
[10] A. Andriotis, M. Menon, D. Srivastava, L. Chernozatonskii, Phys. Rev. Lett. 87 (2001) 066802.
[11] H.Q. Xu, Appl. Phys. Lett. 78 (2001) 2064.
[12] A. Andriotis, M. Menon, D. Srivastava, L. Chernozatonskii, Appl. Phys. Lett. 79 (2001) 266.
[13] S. Reitzenstein, L. Worschech, P. Hartmann, M. Kamp, A. Forchel, Phys. Rev. Lett. 89 (2002) 226804.
[14] T. Müller, A. Lorke, Q.T. Do, F.J. Tegude, D. Schuh, W. Wegscheider, Solid-State Electron. 49 (2005) 1990.
[15] A.M. Song, M. Missous, P. Omling, A.R. Peaker, L. Samuelson, W. Seifert, Appl. Phys. Lett. 83 (2003) 1881.
[16] A. Song, M. Missous, P. Omling, I. Maximov, W. Seifert, L. Samuelson, Appl. Phys. Lett. 86 (2005) 042106.
[17] J. Mateos, B. Vasallo, D. Pardo, T. Gonzalez, Appl. Phys. Lett. 86 (2005) 212103.
[18] C. Balocco, M. Halsall, N.Q. Vinh, A.M. Song, J. Phys.: Condens. Matter 20 (2008) 384203.
[19] A.D. Wieck, K. Ploog, Appl. Phys. Lett. 56 (1990) 928.
[20] J. Nieder, A.D. Wieck, P. Grambow, H. Lage, D. Heitmann, K. von Klitzing, K. Ploog, Appl. Phys. Lett. 57 (1990) 2695.
[21] K.Y. Xu, X.F. Lu, G. Wang, A.M. Song, IEEE T. Nanotechnol. 7 (2008) 451.
[22] D. Reuter, C. Werner, A.D. Wieck, S. Petrosyan, Appl. Phys. Lett. 86 (2005) 162110.
[23] A.S. Achoyan, A.E. Yesayan, E.M. Kazaryan, S.G. Petrosyan, Semiconductors 36 (2002) 903.
[24] D.B. Chklovskii, B.I. Shklovskii, L.I. Glazman, Phys. Rev. B 46 (1992) 4026.